CHAPTER VII
PREPARATION AND STUDY OF SERICIN-G-PLA CLAY AEROGEL WITH ACRYLIC ACID ASSISTED BY PLASMA TECHNIQUE FOR ETHYLENE ADSORPTION APPLICATION

7.1 ABSTRACT

In this research, the study of clay aerogels successfully prepared by freeze-drying was examined for the improvement of its mechanical properties and ethylene adsorption ability. Sericin-g-PLA, having a PLA content of 92-98 wt% and acrylic acid at 4 wt%, were combined with clay dispersion in order to improve mechanical behavior in the aerogel. The plasma technique was used to crosslink acrylic acid. Compression test and dynamic mechanical analysis (DMA) results showed that the Young's modulus of the 6 wt% clay aerogel was 10 kPa while those of the sericin-g-PLA clay aerogels were enhanced from 116 to 296 kPa with an increase in PLA contents from 92 to 98 wt%. In addition, the storage and loss modulus were increased from 3.8 to 12.3 MPa and from 0.3 to 1.4 MPa, respectively. The SEM images of the internal structure of the aerogels showed open pores of aerogels. When sericin contents increase from 2 to 8 wt%, the specific surface area of sericin-g-PLA clay aerogel was increased. Furthermore, the GC measurement revealed that the ability to adsorb ethylene gas in the clay aerogel was 201 ppm/g and the sericin-g-PLA clay aerogels increased from 238 to 462 ppm/g with an increase in sericin content from 2 to 8 wt%.

Keywords: Clay aerogel; Mechanical properties; Ethylene adsorption

7.2 INTRODUCTION

Quality of fruit and vegetable products during handling and storage is maintained by utilizing or modifying practices recommended for fresh produce. Research studies have shown benefits of vacuum cooling (Friedman, 1951), low temperature (Sugawara *et al.*, 1987), and modified atmospheres (Wolfe and Robe,

1980) for prepackaged spinach, cole slaw, shredded lettuce or mixed salad. Use of washing or chemical treatments to remove exposed cellular components or specific cutting tools to minimize damage has been helpful for shredded lettuce (Bolin *et al.*, 1977). These practices do not remove ethylene, a natural ripening initiator that is produced by fruits and vegetables. Ethylene is used commercially to ripen climacteric fruits, such as bananas, tomatoes, honeydew melons, and avocados. Since it induces loss of green color (chlorosis), abscission, and softening, commercial storage rooms should have equipment to remove ethylene when potential problems exist (Watada, 1986). As fruit and vegetable products are placed in sealed packages, ethylene can accumulate and cause undesirable quality changes.

Clay aerogels and clay aerogel/polymer composites are forms of ice templated materials that represent a relatively new family of low density materials. The use of water soluble polymers and sodium montmorillonite can create materials with properties similar to typical foamed polymers. Clay aerogel composites typically have a lamellar structure with layer thicknesses of 1–5 mm and distances between layers of 20–100 mm, which in turn provides for low densities (0.05–0.1 $g \cdot cm^{-3}$) and high porosity (void fraction of ca. 95%). It has been reported that the microscale structure of a unidirectional version of these materials can be controlled by changing the molecular weight of the polymers used and freezing rates (Matthew *et al.*, 2009). Furthermore, the functional groups of copolymers are affected to the properties of composites such as efficient adsorbents of heavy metal cations or dyes (Bulut *et al.*, 2009, Kaplan *et al.*, 2011).

In this study, the sericin-g-PLA clay aerogel with acrylic acid was prepared by freeze-drying and varied the mass ratio between sericin and PLA in sericin-g-PLA in order to study the effect of the mass ratio between sericin and PLA on the properties of the aerogels and also ethylene adsorption ability. The aerogels were studied on morphology, surface area, mechanical, mechanical-thermal, and thermal properties by using SEM, surface area analyzer, universal testing machine, DMA, and TG-DTA, respectively. Moreover, the ethylene adsorption ability of the aerogels was investigated by Gas Chromatography (GC).

7.3 EXPERIMENTAL

7.3.1 Materials

Silk cocoon (*Bombyx mori*); Nang Lai (NL) was purchased from local sericulture in Thailand. Sodium-bentonite was supported from Thai Nippon Co.,Ltd, Thailand. The bentonite is a commercial sodium activated bentonite (Mac-Gel© (GRADE SAC)) with cationic exchange capacity (CEC) of 49.74 meq/100 g clay and used without extra modification. L-lactide monomer (CAS No. 4511-42-6) (99.5% purity) was purchased from Shenzhen Brightchina Induatrial Co., Ltd. Stannous (II) octoate (CAS No. 301-10-0) used as catalyst was purchased from Sigma Aldrich Corp., Japan. Acrylic acid (AA) (CAS No. 79-10-7) used as cross-linked agent was purchased from Sigma Aldrich Corp., USA with molecular weight 72.06 g/mol.

7.3.2 Extraction of Silk Sericin

Silk sericin was extracted by using hot water degumming process. Silk cocoons were rinse with water to eliminate contaminated matter. 20 g of silk cocoons were cut into small pieces (about 5×5 mm^2) and mixed with 300 ml of purified water. Silk cocoons were autoclaved under pressure of 0.8-0.9 atm at 120 °C for 60 min. The silk fiber (fibroin) was filtered out to obtain the sericin aqueous solution. Then, Silk sericin solution was frozen in the glass shells at -40 °C for 12 hr and this glass shell was attached in a freeze-dryer maintained at -110 °C for 48 hr under vacuum to obtain silk sericin powder.

7.3.3 Preparation of Sericin-g-PLA

Stannous (II) octoate ($Sn(Oct)_2$) (0.2 wt%) was added into sericin (Nang Lai) powder (2, 4, 6 and 8 wt%). Then, they were mixed with lactide monomers (98, 96, 94 and 92 wt%, respectively) and stirred at 400 rpm, 140 °C for 10 hr. After 10 hr of mixing, the mixture was cooled down to the room temperature to get the sericin-g-PLA. Then, sericin-g-PLA was grinded into powder.

7.3.4 Preparation of Clay Aerogel

Sodium-bentonite was dispersed in purified water under constant stirring for 3 hr. Then, the gel was immediately frozen in cylindrical glass shells at -40 °C

for 12 hr and attached to a freeze-dryer maintained at -110 °C for 48 hr to sublime the ice out.

7.3.5 Preparation of Sericin-g-PLA Clay Aerogel

Sericin-g-PLA powder (5 wt%) was dispersed in purified water for 1 hr and added into the dispersed Na-bentonite under constant stirring followed by continuous stirring for 2 hr. Then, the gel was immediately frozen in cylindrical glass shells at -40 °C for 12 hr and attached to a freeze-dryer maintained at -110 °C for 48 hr to sublime the ice out.

7.3.6 Preparation of Sericin-g-PLA Clay Aerogel with Acrylic Acid

Sericin-g-PLA powder (5 wt%) was dispersed in purified water and mixed with acrylic acid for 1 hr. The mixture was added into the dispersed Na-bentonite under constant stirring followed by continuous stirring for 2 hr. After that the gel was treated by plasma in air and stirred for 15 min. Then, the gel was immediately frozen in cylindrical glass shells at -40 °C for 12 hr and attached to a freeze-dryer maintained at -110 °C for 48 hr to sublime the ice out.

7.3.7 Characterizations

7.3.7.1 Thermogravimetric-Differential Thermal Analyner (TG-DTA)

Thermal stability of sericin-g-PLA clay aerogel with acrylic acid was examined by PERKIN-ELMER Pyris Daimond thermogravimetric analysis. The weight of sample was in the range of 5-7 mg and heated at the heating rate of 10 °C/min from 50-800 °C in nitrogen atmosphere with 20 ml/min of nitrogen flow rate.

7.3.7.2 Universal Testing Machine

The Young's modulus of sericin-g-PLA clay aerogel with acrylic acid was investigated by LLOYD Lrx Universal Testing Machine in compression mode with 500 N load cell at constant crosshead speed of 1 mm/min. The aerogels were prepared in the cylindrical shape with ~20 mm in diameter and height. Five samples of each composition were tested for reproducibility. The compressive modulus was calculated from the slope of the linear portion of the stress-strain curve.

7.3.7.3 Dynamic Mechanical Analysis (DMA)

DMA analyze was carried out by using a dynamic-mechanical analyzer GABO EPLEXOR QC 25 instrument. The testing temperature was set from -50 to 150 °c, heating rate 2 °C/min, 1 Hz for frequency. The aerogels were prepared in the

cylindrical shape with ~20 mm in diameter and height. The compression mode was used.

7.3.7.4 Scanning Electron Microscroscopy (SEM)

The morphology of sericin-g-PLA clay aerogel with acrylic acid was observed by using TM 3000 Scanning Electron Microscope. The samples were fixed on stubs with carbon tape and coated with platinum under vacuum. SEM micrographs were taken with low magnification at 40 and high magnification at 40.0 k using an accelerator voltage of 15 kV.

7.3.7.5 Gas Chromatography (GC)

The ethylene adsorption ability of the aerogels was investigated by using MODEL 910 GAS CHROMATOGRAPH (GC). The aerogels were prepared in the cylindrical shape with ~20 mm in diameter and ~30 mm in height. A 1 mL calibration ethylene gas spanning the concentration range from 1000 to 6000 g mL^{-1} was injected into the GC. A standard curve was then made by plotting the peak area versus the concentration injected. The ethylene concentration of the analyte was calculated according to the standard curve.

7.3.7.6 Surface Area Analyzer

The surface area of the aerogels was analyzed by Quantachrome (Autosorb-1) instrument. The samples were weight about 0.07-0.08 g into the sample tube and degassed at 150 °C overnight under vacuum and nitrogen trap. The sample was analyzed at 150 °C and nitrogen was used as an adsorbent gas.

7.3.7.7 Swelling Behavior

The swelling behavior of sericin-g-PLA clay aerogel with acrylic acid was studied by using conventional gravimetric procedure. The sample was dried in an oven at 60 °C over night and weighed to obtain weight of dry sample (W_1). The dry sample was immersed in water at 25 °C for 24 hr. The swollen sample was withdrawn, wiped to remove the excess water out, and reweighed (W_2). The swelling percentage was calculated as shown in Eq. 7.1.

$$swelling\ percentage = \frac{W_2 - W_1}{W_1} \times 100 \quad (Eq.7.1)$$

7.3.7.8 Density Measurement

The density of the aerogels was determined by mass and dimension measurement according to an equation:

$$\rho = \frac{M}{V} \quad (Eq. 7.2)$$

where ρ is mass density (g/cm^3), M is mass of sample (g) and V is volume of sample (cm^3). Mass and volume was measured using Sartorius BS 224 S analytical balance and digital vernier caliper.

7.4 RESULTS AND DISCUSSION

7.4.1 Thermal Stability of Sericin-g-PLA Clay Aerogel with Acrylic Acid

The thermal stability of sericin-g-PLA clay aerogel with acrylic acid is shown in Figure 7.1. The loss in mass started at 130 °C, which is due to non-cross-linked acrylic acid and evaporation of water (Horia and Abdel, 2012). The weight loss that starting from 240 to 350 °C was associated to anhydride formation and decarboxylation processes of poly(acrylic acid) (Mohamed *et al.*, 2012). Moreover, this step was associated with the decomposition of sericin (Nang Lai, NL) and PLA which around 255 °C and 251 °C, respectively. When considered the mass ratio between sericin and PLA in sericin-g-PLA, decreasing PLA content result in decreased the decomposition onset temperature. According to the previous results in CHAPTER V, the decrease of PLA content results in the decrease of weight average molecular weight (Mw) of sericin-g-PLA. Zhang *et al.* (1992) reported that the decomposition temperature range depends on the polymer's molecular weight. The higher of molecular weight showed the higher of decomposition temperature.

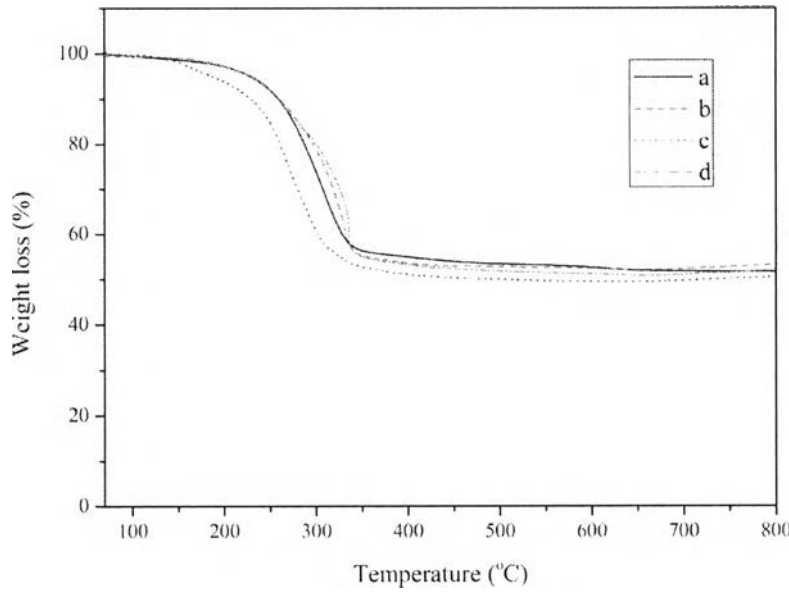

Figure 7.1 TGA curves of sericin-g-PLA clay aerogel with acrylic acid (a) NL2PLA98, (b) NL4PLA96, (c) NL6PLA94, and (d) NL8PLA92 (acrylic acid 4 wt%, plasma treatment time 30 s and clay 6 wt%).

Table 7.1 Thermal stability of sericin-g-PLA clay aerogel with acrylic acid with various mass ratio between sericin and PLA (acrylic acid 4 wt%, plasma treatment time 30 s and clay 6 wt%)

Mass ratio (sericin:PLA)	**T_d onset (°C)**	**Weight loss (%)**
2:98	257.5	45.8
4:96	254.0	46.5
6:94	225.0	49.8
8:92	221.2	47.7

7.4.2 Mechanical Properties

The compressive properties of sericin-g-PLA clay aerogel with acrylic acid are characterized by using Lloyd universal testing machine. The compressive stress-strain curves of the aerogels are shown in Figure 7.2. Table 7.2 summarized

the mechanical properties of sericin-g-PLA clay aerogel with acrylic acid. The results showed that increasing of PLA content from 92 to 98 wt% in sericin-g-PLA, the Young's modulus increased from 116 to 296 kPa. These indicate that PLA presents a high modulus that affects to the Young's modulus of the aerogel (Auras *et al.*, 2004).

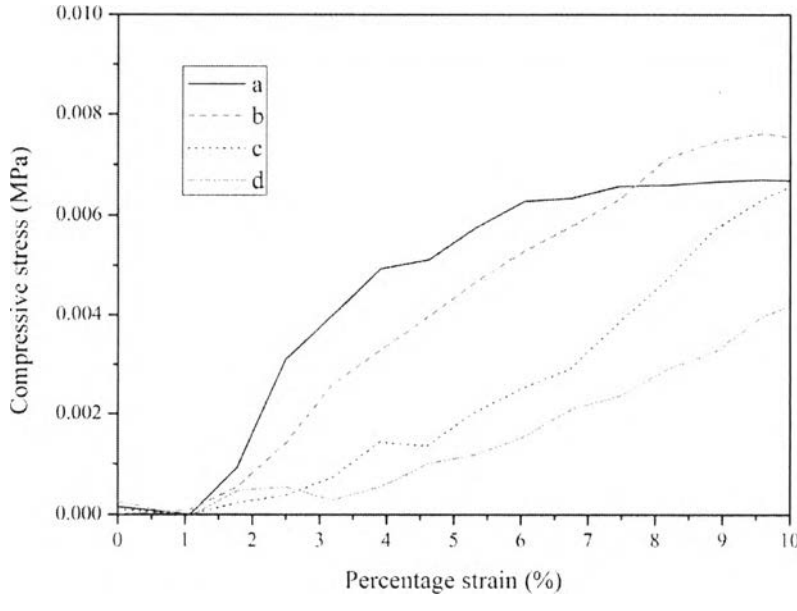

Figure 7.2 Stress-strain curves of sericin-g-PLA clay aerogel with acrylic acid (a) NL2PLA98, (b) NL4PLA96, (c) NL6PLA94, and (d) NL8PLA92 (acrylic acid 4 wt%, plasma treatment time 30 s and clay 6 wt%).

Table 7.2 Effect of mass ratio of sericin (NL) and PLA on mechanical properties of NL-g-PLA clay aerogel with acrylic acid

Mass Ratio (sericin:PLA)	**Young's modulus (kPa)**	**Stiffness (kN/m^2)**
2:98	296.45±65.12	3.10±0.35
4:96	232.19±31.54	2.43±0.33
6:94	150.77±23.21	1.58±0.24
8:92	115.89±33.12	1.21±0.33

7.4.3 Dynamic Mechanical Properties

The dynamic mechanical properties are characterized by using a dynamic-mechanical analyzer GABO EPLEXOR QC 25 instrument. The storage modulus and loss modulus of copolymers which depend on temperature are shown in Figure 7.3 to 7.4. The results showed that increasing of PLA content from 92 to 98 wt% in sericin-g-PLA, the storage and loss modulus were increased from 3.8 to 12.3 MPa and from 0.3 to 1.4 MPa, respectively. The difference in storage modulus of the aerogel results in the difference of stiffness. These indicate that the aerogel has the highest of stiffness on the maximum of PLA content (Sriya *et al.*, 2013).

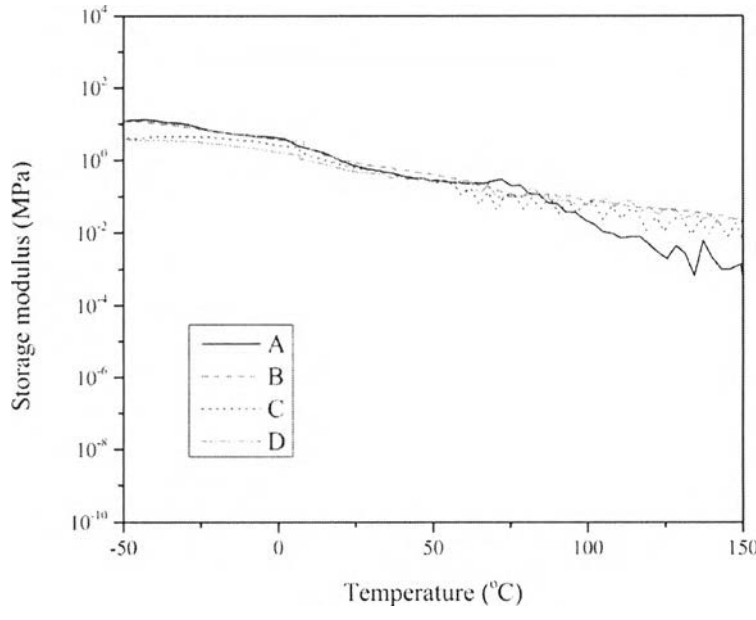

Figure 7.3 The storage modulus of sericin-g-PLA clay aerogel with acrylic acid (A) NL2PLA98, (B) NL4PLA96, (C) NL6PLA94, and (D) NL8PLA92 (acrylic acid 4 wt%, plasma treatment time 30 s, and clay 6 wt%).

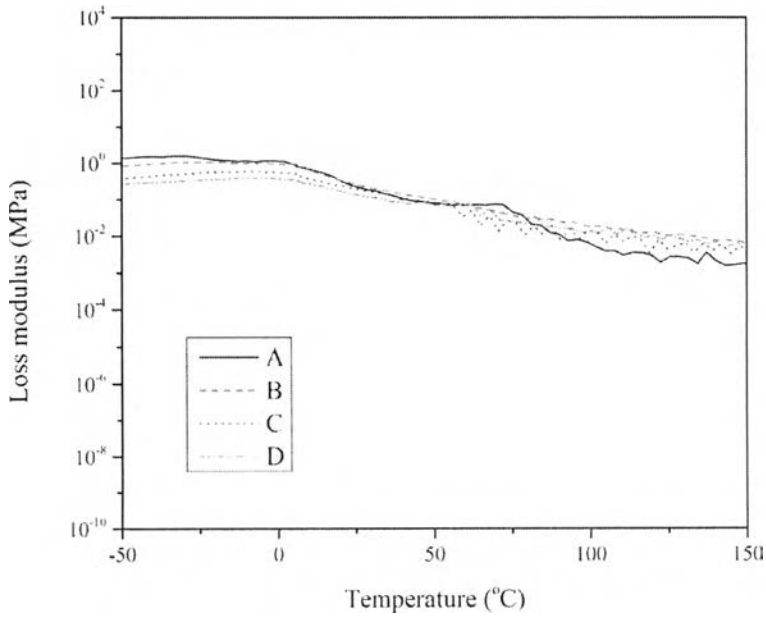

Figure 7.4 The loss modulus of sericin-g-PLA clay aerogel with acrylic acid (A) NL2PLA98, (B) NL4PLA96, (C) NL6PLA94, and (D) NL8PLA92 (acrylic acid 4 wt%, plasma treatment time 30 s, and clay 6 wt%).

7.4.4 Morphology of the Aerogels

The SEM micrograph of neat Na-bentonite aerogel is shown in Figure 7.5. After freeze-drying, neat Na-bentonite formed the lamella structure which was duplicate of the ice crystal morphology (Gawryla *et al.*, 2008). Moreover, the porous structure was visibly observed in the freeze-dried clay aerogel. The sericin-g-PLA clay aerogel, having a PLA content of 98 wt% and sericin at 2 wt%, as shown in Figure 7.6, showed the lamella morphology similar to clay aerogel but the clay layers were covered by sericin-g-PLA.

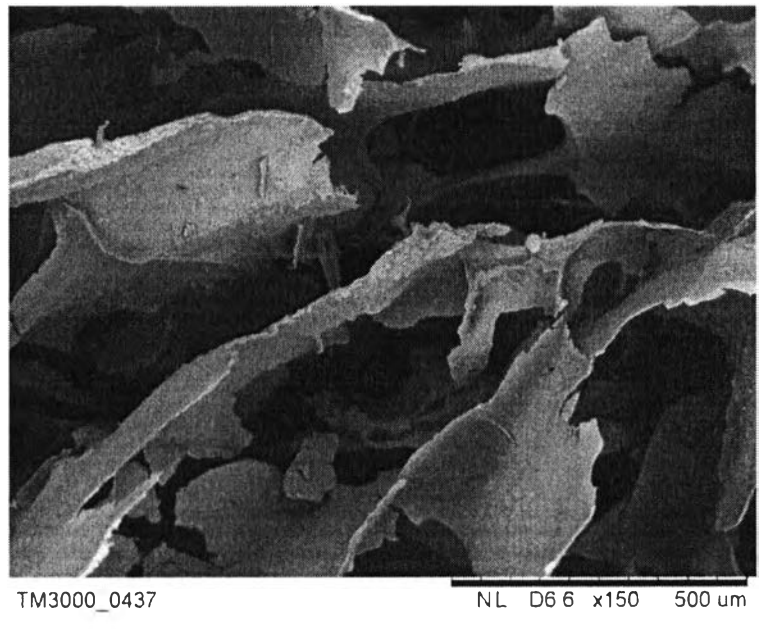

Figure 7.5 SEM micrograph of 6 wt% of clay aerogel.

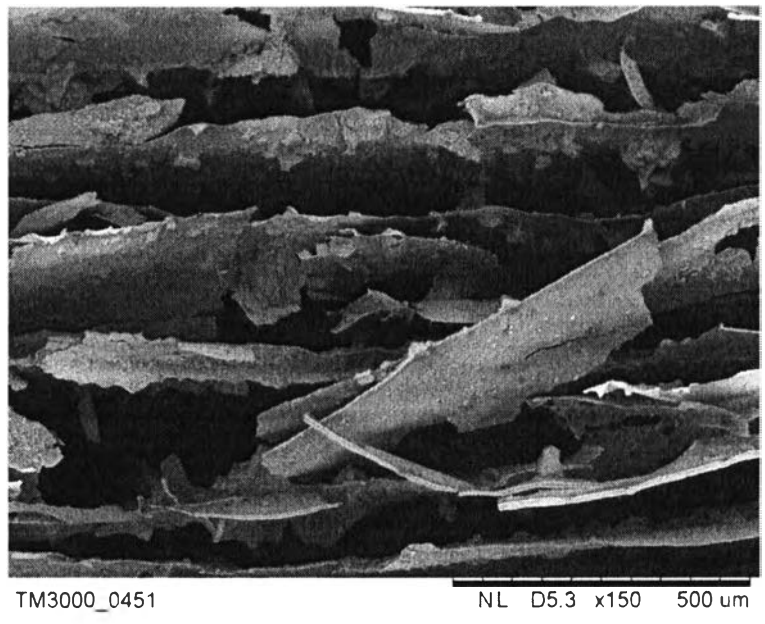

Figure 7.6 SEM micrograph of 6 wt% of clay aerogel with 5 wt% of sericin-g-PLA.

The sericin-g-PLA clay aerogel with acrylic acid showed the lamella morphology. The SEM micrographs are shown the high porosity (Figure 7.7). Figure 7.8 shows the surface of the clay layers that confirmed the covered clay layers by sericin-g-PLA. The porous structure was the important characteristics of porous adsorbents (Hwang et al., 2010). These are the important motive to apply this aerogel into the ethylene adsorption application.

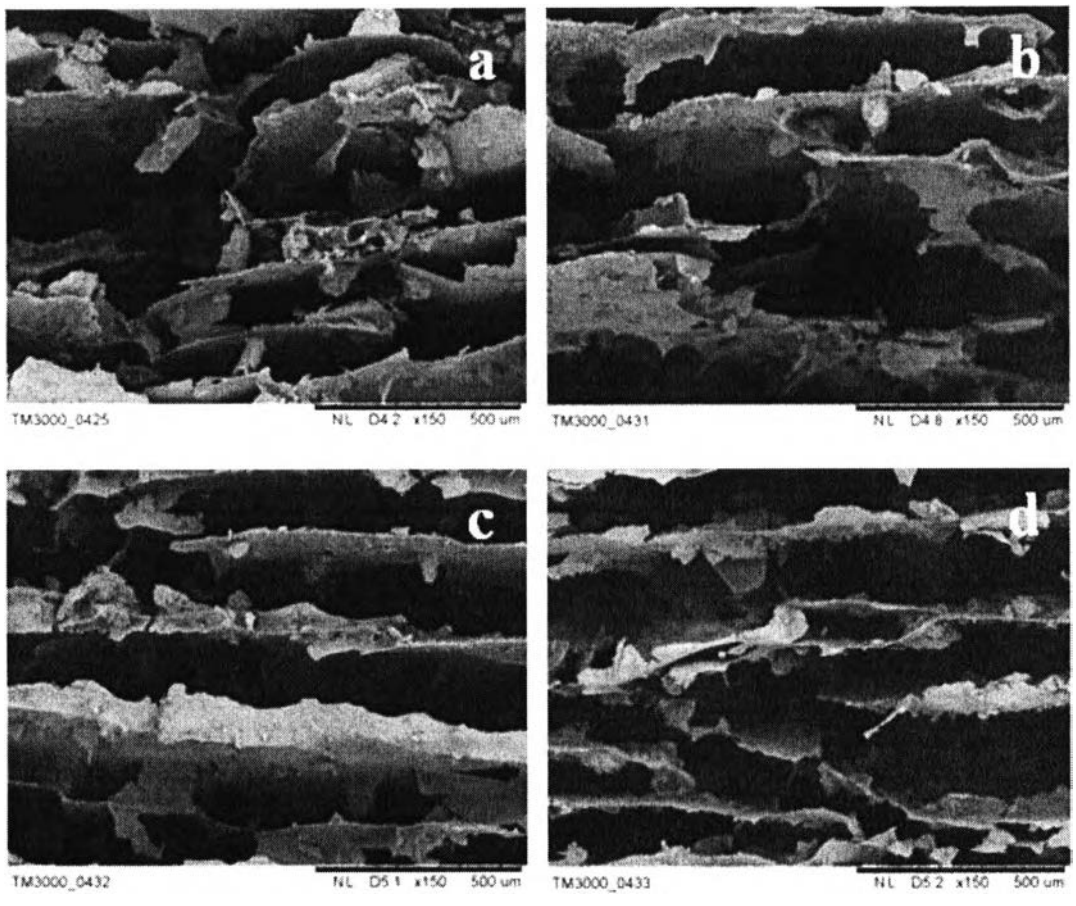

Figure 7.7 SEM micrograph of sericin-g-PLA clay aerogel with acrylic acid (a) NL2PLA98, (b) NL4PLA96, (c) NL6PLA94, and (d) NL8PLA92 (acrylic acid 4 wt%, plasma treatment time 30 s, and clay 6 wt%).

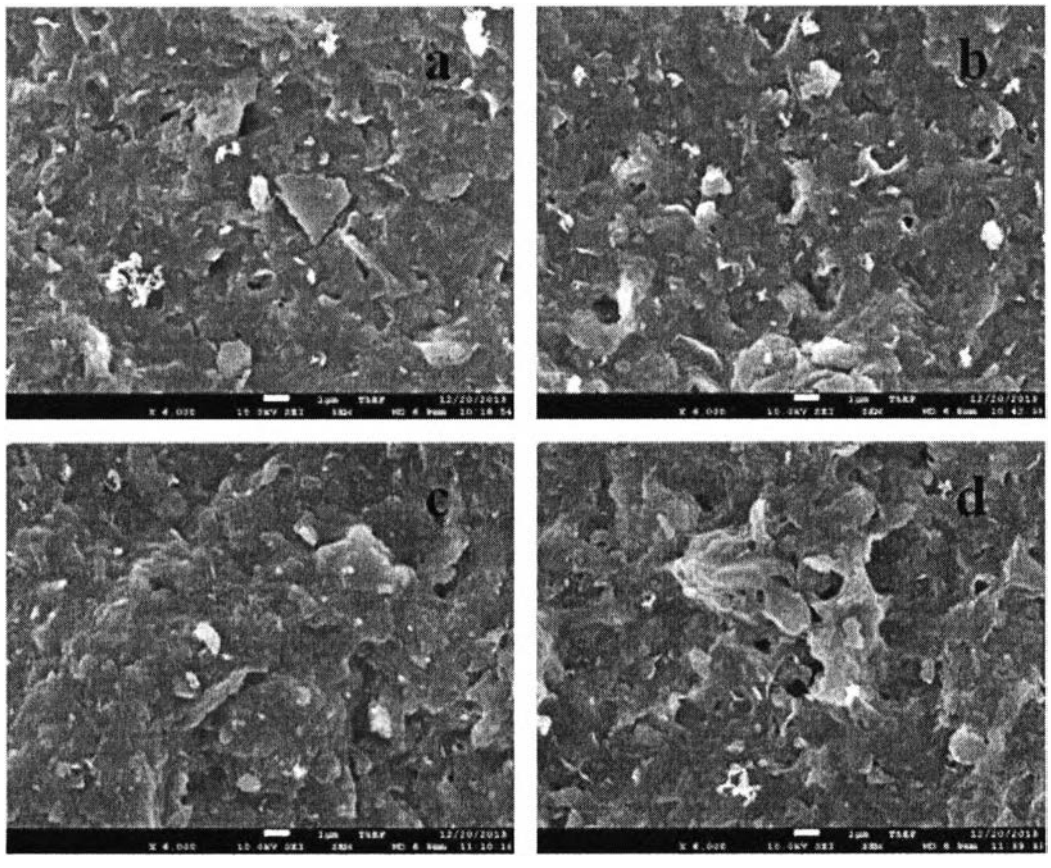

Figure 7.8 FE-SEM micrograph of sericin-g-PLA clay aerogel with acrylic acid (a) NL2PLA98, (b) NL4PLA96, (c) NL6PLA94, and (d) NL8PLA92 (acrylic acid 4 wt%, plasma treatment time 30 s, and clay 6 wt%).

7.4.5 Ethylene Adsorption Ability

The ethylene adsorption ability of the aerogels was investigated by using MODEL 910 GAS CHROMATOGRAPH (GC). The aerogels were prepared in the cylindrical shape with ~20 mm in diameter and ~30 mm in height that showed in Figure 7.9. Figure 7.10 presents ethylene adsorption of silk sericin, 6 wt% of clay aerogel and 6 wt% of clay aerogel with 5 wt% of sericin-g-PLA as a function of time. Silk sericin shows the high ability to adsorb the ethylene gas that corresponded to the high amino groups which was confirmed by FTIR spetra in CHAPTER IV. Clay aerogel showed an abrupt increase in ethylene absorption (about 840 ppm/g) then drop off at the very beginning stage followed by the gradual decrease of ethylene absorption. This indicates that due to its high pore volume, the clay areogel

can instantaneously accommodate large amount of ethylene but with its limited active sites, ethylene is thus gradually released afterward. The clay aerogel is thus more likely to behave as a controlled-released device. Its ethylene absorption after 10 days was found to be 201 ppm/g. Moreover, the addition of sericin-g-PLA, having a PLA content of 98 wt% and sericin at 2 wt%, gives the high ability to adsorb the ethylene gas compared to the neat clay aerogel. This suggests that the amino groups in sericin-g-PLA effectively bind to ethylene similar to amine adsorption of carbon dioxide (Reine and Eldridge, 2005). The reaction of ethylene adsorption of sericin was shown in Figure 7.11. The resulting ethylene adsorption was due to chemical complexation with serine.

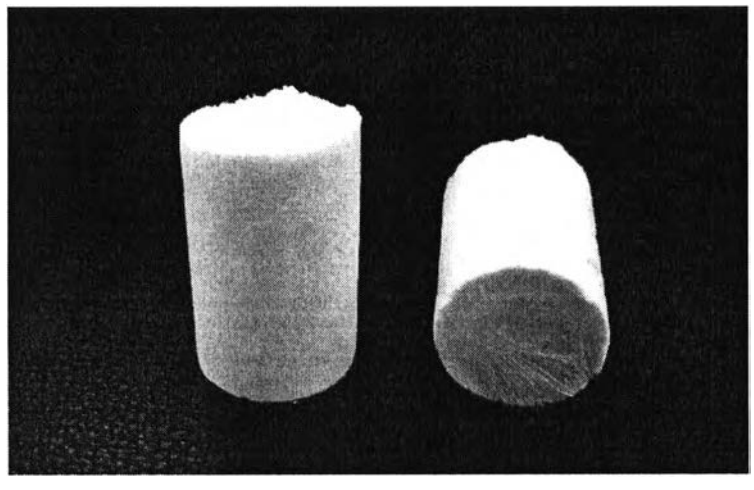

Figure 7.9 Appearance of the aerogels.

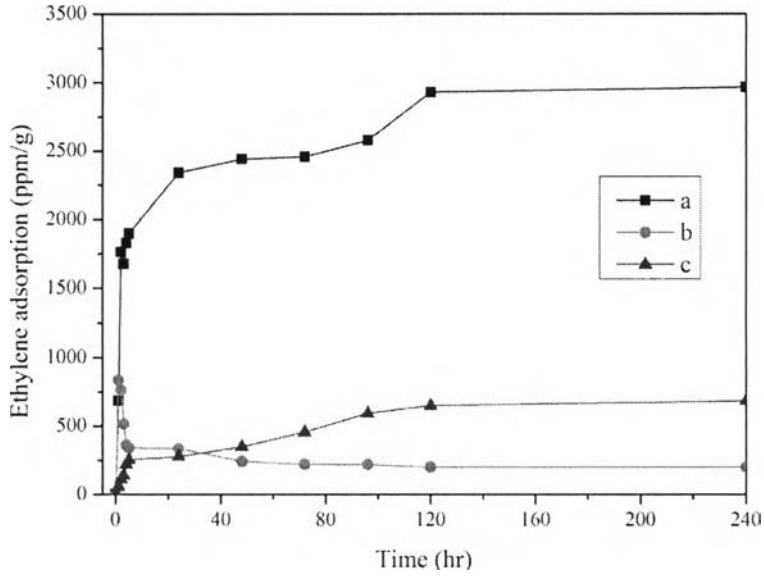

Figure 7.10 Ethylene adsorption of (a) silk sericin, (b) 6 wt% of clay aerogel, and (c) 6 wt% of clay aerogel with 5 wt% of sericin-g-PLA.

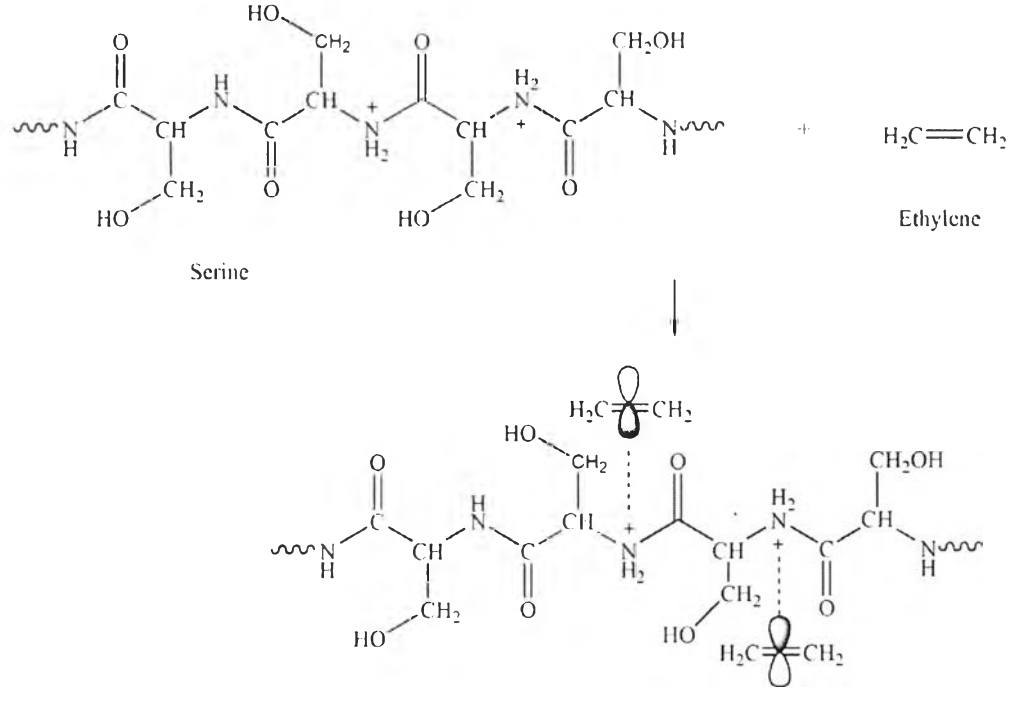

Figure 7.11 Purposed ethylene adsorption mechanism.

Ethylene adsorption of sericin-g-PLA clay aerogel with acrylic acid was shown in Figure 7.12. The idea of grafting functional groups onto the pore walls of materials is a known strategy for the design of promising new adsorbents (Hwang et al., 2010). In addition, modifications in the surface chemistry of the porous materials by incorporating basic sites capable of interacting strongly with ethylene in order to increase ethylene adsorption ability and to keep high selectivity for ethylene are considered very promising (Arunkumar et al., 2012). The different sericin contents in sericin-g-PLA are affected to ethylene adsorption ability of the aerogels. When sericin content increased, the ethylene adsorption ability of the aerogels was increased. This indicates that raising sericin content in sericin-g-PLA results in the increase of amino groups leading to greater ethylene adsorption ability.

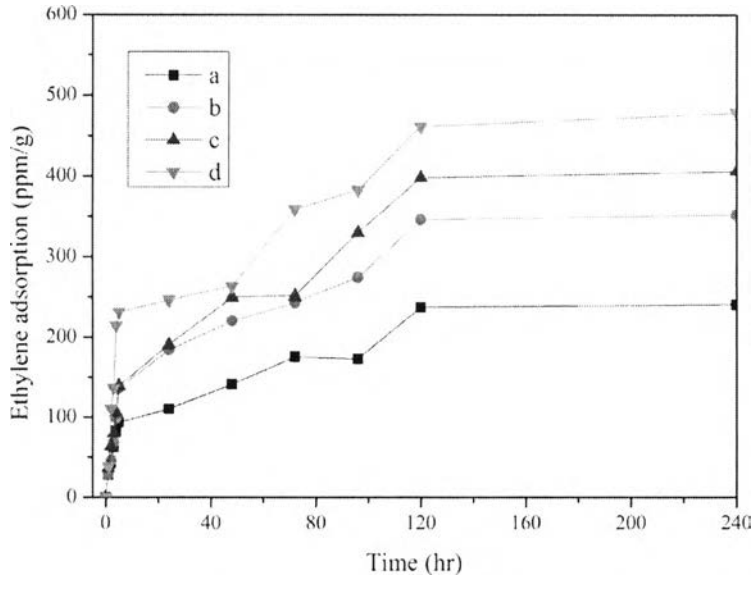

Figure 7.12 Ethylene adsorption of sericin-g-PLA clay aerogel with acrylic acid (a) NL2PLA98, (b) NL4PLA96, (c) NL6PLA94, and (d) NL8PLA92 (acrylic acid 4 wt%, plasma treatment time 30 s, and clay 6 wt%).

7.4.6 The Specific Surface Area Measurement

The Brunauere-Emmette-Teller (BET) specific surface area and the total pore volume per mass unit as determined from the adsorption isotherms for the aerogels. If the quantity of an adsorbing gas on a surface is measured over a wide

range of relative pressures at a constant temperature, an adsorption isotherm is obtained. Similarly, desorption isotherms can be derived by measuring the quantities of gas removed from the surface, when the relative pressure is lowered. According to Brunauer *et al.* (1940), adsorption isotherms can be grouped into five types. For Figure 7.13 and 7.14, the adsorption and desorption isotherms of 6 wt% of clay aerogel and sericin-g-PLA clay aerogel with acrylic acid were classified into type IV. Type IV isotherm exhibits a steep slope at higher pressures and hysteresis due to capillary condensation in mesopores (pore diameter of 20 – 500 Å). Table 7.3 shows the BET specific surface area and the total pore volume per mass unit of the aerogels. When compared to the clay aerogel, the incorporation of clay leads to lower BET surface area (Jiao *et al.*, 2013). The specific surface area of sericin-g-PLA clay aerogel with acrylic acid increases significantly from 12.51 to 18.17 $m^2 g^{-1}$ with an increase of sericin content from 2 to 8 wt%. For a mixture of clay and organic components, the informative value of BET-N_2 specific surface area is restricted. Since the nitrogen molecule acts as a polar probe, hydrophobic regions of organic material will not be covered and thus, nitrogen adsorbs to only a small portion of the organic material, possibly its external part of the surface area. Consequently, it is likely that BET-N_2 specific surface area values underestimate the specific surface area of the organic material. Moreover, the clay and organic components interact with each other. They can be glued together to form microaggregates or coatings on clay surfaces can develop. However, it has been shown that the coating by organic material does not occur homogeneously but rather in distinct patches. These patches of organic material are likely located at the entrance of pores, thereby impeding the entrance of nitrogen molecules into these pores (Katja, 2014).

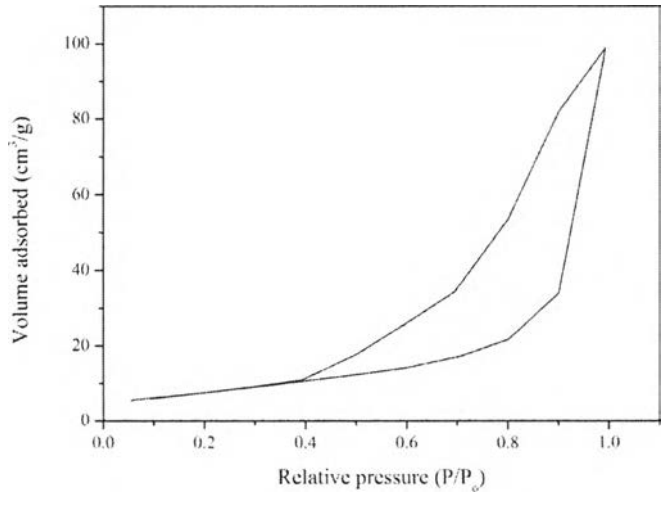

Figure 7.13 The adsorption and desorption isotherms of 6 wt% of clay aerogel.

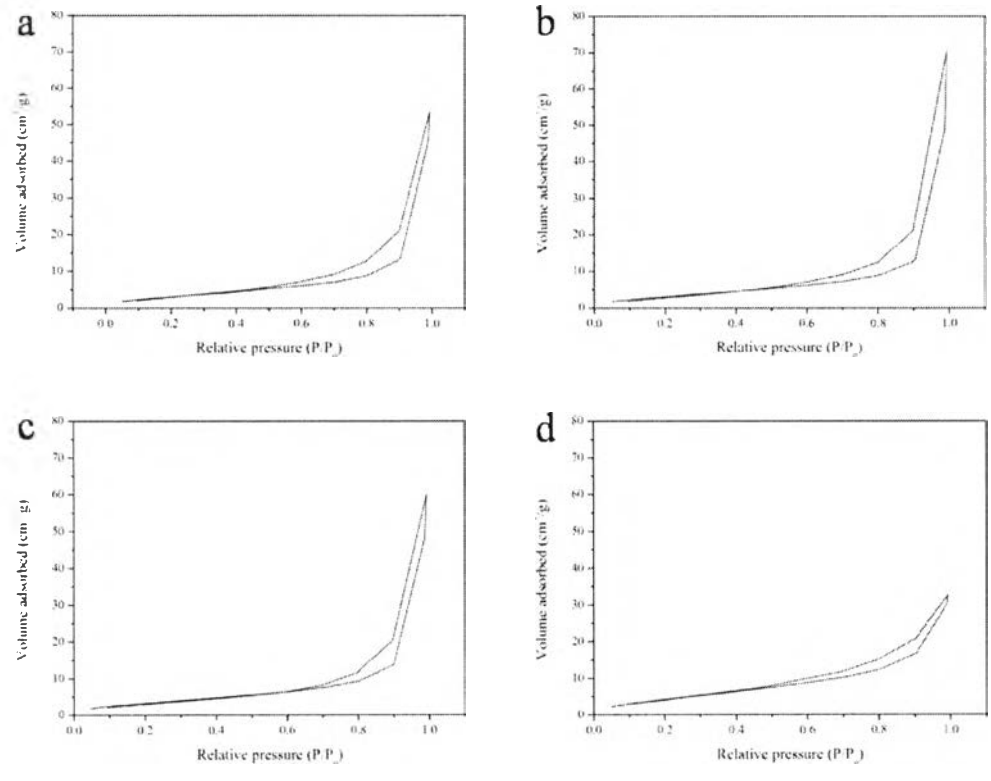

Figure 7.14 The adsorption and desorption isotherms of sericin-g-PLA clay aerogel with acrylic acid (a) NL2PLA98, (b) NL4PLA96, (c) NL6PLA94, and (d) NL8PLA92 (acrylic acid 4 wt%, plasma treatment time 30 s, and clay 6 wt%).

Table 7.3 The BET specific surface area and pore volume of the clay aerogels and sericin-g-PLA clay aerogel with acrylic acid with various mass ratios between sericin and PLA

Sample	BET specific surface area ($m^2 g^{-1}$)	Pore volume ($cm^3 g^{-1}$)
Clay aerogel 6 wt%	28.55	0.146
NL2PLA98	12.51	0.070
NL4PLA 96	12.95	0.076
NL6PLA94	13.46	0.075
NL8PLA92	18.17	0.046

7.4.7 Swelling Behavior

Swelling studies of sericin-g-PLA clay aerogel with acrylic acid showed in Figure 7.15. The minimum swelling percentage was observed in clay aerogel with sericin-g-PLA contained 8 wt% of sericin and 92 wt% of PLA. The network of sericin-g-PLA and acrylic acid formed from the chemical cross-linked by plasma initiation was hold the clay bundle and limited the swelling of the clay aerogels. This indicates that the highest cross-linked degree led to the lowest of swelling percentage.

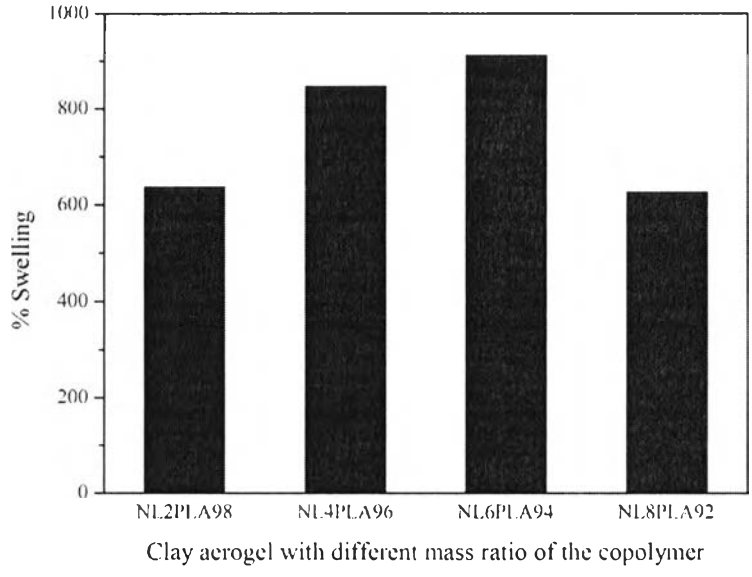

Figure 7.15 The swelling percentage of sericin-g-PLA clay aerogel with acrylic acid (a) NL2PLA98, (b) NL4PLA96, (c) NL6PLA94, and (d) NL8PLA92 (acrylic acid 4 wt%, plasma treatment time 30 s, and clay 6 wt%).

7.4.8 Density

The density of the clay aerogels are showed in Table 7.4. Sericin-g-PLA clay aerogels with acrylic acid presented the closed density ranged between 0.10 to 0.11 g/cm^3 depended on the composition of the aerogels. Moreover, increasing of sericin content in sericin-g-PLA was not outstandingly affected on the density of the aerogels.

Table 7.4 Density of the clay aerogels

Samples	Density (g/cm^3)
C6 with sericin-g-PLA (NL2PLA98)	0.11±0.004
C6 with sericin-g-PLA (NL4PLA96)	0.11±0.008
C6 with sericin-g-PLA (NL6PLA94)	0.10±0.003
C6 with sericin-g-PLA (NL8PLA92)	0.11±0.002

7.5 CONCLUSIONS

The sericin-g-PLA clay aerogel with acrylic acid were successfully prepared by freeze-drying technique. The sericin-g-PLA and acrylic acid were used to improve the mechanical properties of the clay aerogel. Increasing PLA content in sericin-g-PLA, the decomposition onset temperature and the Young's modulus were increased. Moreover, the sericin content in sericin-g-PLA was affected to the surface area and ethylene adsorption ability but not affected on the density of the aerogels. Increasing of sericin content, the surface area and ethylene adsorption ability of the aerogels were enhanced significantly. The resulting ethylene adsorption was due to chemical complexation with serine.

7.6 ACKNOWLEDGEMENTS

The authors appreciate to thank the Center of Excellence on Petrochemical and Materials Technology and the government budget 2013 for the financial support.

7.7 REFERENCES

Arunkumar, S., An, Z., George, K.H., Partha, S., and Rajender, G. (2012) Post-combustion CO_2 capture using solid sorbents: A review. Ind. Eng. Chem. Res., 51, 1438-1463.

Auras, R., Harte, B., and Selke, S. (2004) An overview of polylactides as packaging materials. Macromolecular Bioscience, 4 , 835–864.

Bolin, H. R., Stafford, A.E., King, A.D., and Huxsoll, C.C. (1977) Factors affecting the storage stability of shredded lettuce. J. Food Sci., 42, 1319-1332.

Brunauer, S., Deming, L.S., Deming,W.E., Teller, E., (1940) On a theory of the van der Waals adsorption of gases. J. Am. Chem. Soc., 62, 1723–1732.

Bulut, Y., Akcay, G., Elma, D., and Serhatlı, I.E. (2009) Synthesis of clay-based superabsorbent composite and its sorption capability. J Hazard Mater., 171, 717–723.

Friedman, B.A. (1951) Vacuum cooling of prepackaged spinach, cole slaw and mixed salad. Proc. Amer. Sot. Hart. Sci., 58, 279-286.

Gawryla, M. D., Nezamzadeh, M., and Schoraldi, D. A. (2008) Foam-like materials produced from abundant natural resources. Green Chemistry, 10, 1078-1081.

Horia, M. M., and Abdel, W. M. (2012) Radiation synthesis of acrylic acid/polyethyleneimine interpenetrating polymer networks (IPNs) hydrogels and its application as a carrier of atorvastatin drug for controlling cholesterol, European Polymer Journal, 48, 1632-1640.

Hwang, K., Son, Y., Park, S., Park, D., Oh, K., and Kim, S. (2010) Adsorption of carbon dioxide onto EDA-CP-MS41. Separation Science and Technology, 45, 85-93.

Jiao, G., Baochau, N., Lichun, L., Mary, A., Daniel, A., and Miko, C. (2013) Clay reinforced polyimide/silica hybrid aerogel. J. Mater. Chem. A, 1, 7211-7221.

Kaplan, M., and Kasgoz, H. (2011) Hydrogel nanocomposite sorbents for removal of basic dyes. Polym Bull., 67, 1153–1168.

Katja, H. (2014) The measurement of the specific surface area of soils by gas and polar liquid adsorption methods—Limitations and potentials. Geoderma, 2014, 75-87.

Matthew, D.G., Lei, L., Jaime, C.G., and David, A.S. (2009) pH tailoring electrical and mechanical behavior of polymer–clay–nanotube aerogels. Macromol. Rapid Commun., 30, 1669-1673.

Ren, C.S., Wang, D.Z., and Wang, Y.N. (2006) Graft co-polymerization of acrylic acid onto the linen surface induced by DBD in air. Surface & Coatings Technology, 201, 2867-2870.

Sriya, D., Fahmida, I., Lan M., Sanjoy, K.B., Ronald, C.H., and Micah, J.G. (2013) Rheology and morphology of pristine graphene/polyacrylamide gels. Acs Appl. Mater. Interfaces, 5, 8633-8640.

Sugawara, W., Kawano, S., Shiina, T., and Ohata, H. (1987) Quality control of shredded lettuce during preservation and distribution. J. Jpm. Soc. Cold Preservation Food, 13, 92-99.

Watada, A.E. (1986) Effects of ethylene on the quality of fruits and vegetables. Food Technol., 40(5), 82-90.

Wolfe, S.K. and Robe, K. (1980) Modified atmosphere extends precut lettuce shelf life. Food Processing, 41(9), 34-42.

Zhang, X., Wyss, U.P., Pichora, D., and Goosen, M. (1992) An investigation of the synthesis and thermal stability of poly(DL-lactide). Polymer Bulletin, 27, 623-629.